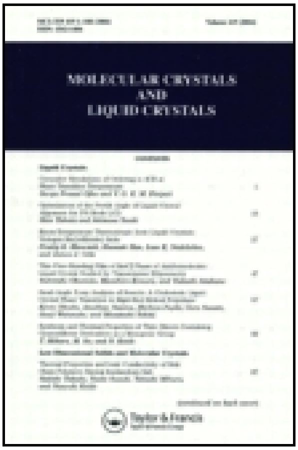

Molecular Crystals and Liquid Crystals Science and Technology. Section A. Molecular Crystals and Liquid Crystals
Publication details, including instructions for authors and subscription information:
http://www.tandfonline.com/loi/gmcl19

Molecular Motions in the Novel Plastic Phase of Decamethylferrocene Studied by ^{1}H NMR and Thermal Measurements

T. Kobayashi [a] , H. Ohki [a] & R. Ikeda [a]
[a] Department of Chemistry, University of Tsukuba, Tsukuba, 305, Japan

To cite this article: T. Kobayashi , H. Ohki & R. Ikeda (1994): Molecular Motions in the Novel Plastic Phase of Decamethylferrocene Studied by ^{1}H NMR and Thermal Measurements, Molecular Crystals and Liquid Crystals Science and Technology. Section A. Molecular Crystals and Liquid Crystals, 257:1, 279-287

To link to this article: http://dx.doi.org/10.1080/10587259408033784

Mol. Cryst. Liq. Cryst., 1994, Vol. 257, pp. 279–287
Reprints available directly from the publisher
Photocopying permitted by license only

Molecular Motions in the Novel Plastic Phase of Decamethylferrocene Studied by ^{1}H NMR and Thermal Measurements

T. KOBAYASHI, H. OHKI and R. IKEDA

Department of Chemistry, University of Tsukuba, Tsukuba, 305, Japan

(Received April 2, 1993; in final form January 3, 1994)

The ^{1}H NMR spin-lattice relaxation time and second moment of the resonance line-width in solid decamethylferrocene $[(CH_3)_5C_5]_2Fe$ have been measured in temperature ranges 85–540 K, and 300–540 K respectively. The presence of two solid–solid phase transitions were revealed at 397 ± 1 K and 501 ± 2 K, by differential scanning calorimetry. Phase I obtainable above 501 K was shown to be a plastic phase, where the isotropic molecular rotation and the translational self-diffusion rapidly take place. In the low-temperature Phases II and III, excitations of the CH_3 reorientation, the uniaxial reorientation of the whole molecule about its C_5 axis and the nutation of this C_5 axis were observed.

INTRODUCTION

Dynamic structure and molecular motions in solid metallocene compounds, e.g., ferrocene and its derivatives, ruthenocene, azaferrocene and ferrocenium salts, have extensively been studied by NMR,[1–7] Mössbauer spectroscopy[8–10] and thermal measurements.[11–19] From these studies, structural phase transitions associated with conformation changes of the five-membered ring and large-amplitude motions such as the molecular overall rotation have been observed indicating small intermolecular interaction in crystals of this system. The plastic crystal phase consisting of molecules with the isotropic rotation and the translational self-diffusion has been revealed in formylferrocene[4,8] and tetrachloroferrocene[7,9] in temperature ranges of 317–397 K and 391–420 K, respectively. Solid ferrocene studied in detail,[1,2,5,11–15] has been reported to contain molecules almost freely rotating about the C_5 axis at room temperature. Upon heating, however, no phase transition has been observed up to the melting temperature (T_m) of 446–447 K[20] suggesting no further excitation of large amplitude motions. For decamethylferrocene, $[(CH_3)_5C_5]_2Fe$ having a high symmetric molecular structure analogous to ferrocene, it has been reported that crystals can be heated up to T_m of 564–568 K without decomposition.[21] Our preliminary thermal measurement revealed the presence of phase transitions above room temperature. In the present study, we investigate the dynamic structure of the highly movable molecules in high temperature phases of solid decamethylferrocene.

EXPERIMENTAL

Decamethylferrocene purchased from Strem Chemicals, Inc. was purified by sublimation at 120°C. The obtained fine crystals were dried and placed in a glass ampoule under vacuum, then sealed after putting in a small amount of dry nitrogen gas.

Differential thermal analysis (DTA) was carried out in a temperature range 90–435 K using a homemade apparatus[22] to detect possible phase transitions. Differential scanning calorimetry (DSC) was performed to determine transition enthalpies between room temperature and 625 K using a Seiko Instruments SSC5200 calorimeter. ^{1}H NMR spin–lattice and spin–spin relaxation times, T_1 and T_2, respectively, and the second moment M_2 of the resonance line-width were determined at Larmor frequencies 9.45–45.8 MHz by a home-built pulsed spectrometer constructed with a Thamway A57-4702 wide-band power amplifier, Matec model 251 and 252 preamplifiers, an Anritsu M40570 frequency synthesizer and a Jeol JTR-310 electromagnet. The inversion recovery and Hahn's spin-echo methods were employed to determine T_1 and T_2, respectively. We calculated M_2 values from the recorded echo decay curves. The sample temperature was controlled by the conventional nitrogen gas flow method and determined by a chromel-constantan thermocouple within an accuracy of ± 1 K.

RESULTS

Thermal Measurements (DTA, DSC)

A DSC thermogram measured above room temperature at a heating rate of 5 K min^{-1} is shown in Figure 1. No heat anomaly was observed below room temperature down to ca. 90 K. New phase transitions were detected at 397 ± 1 K(T_{tr2}) and 501 ± 2 K(T_{tr1}).

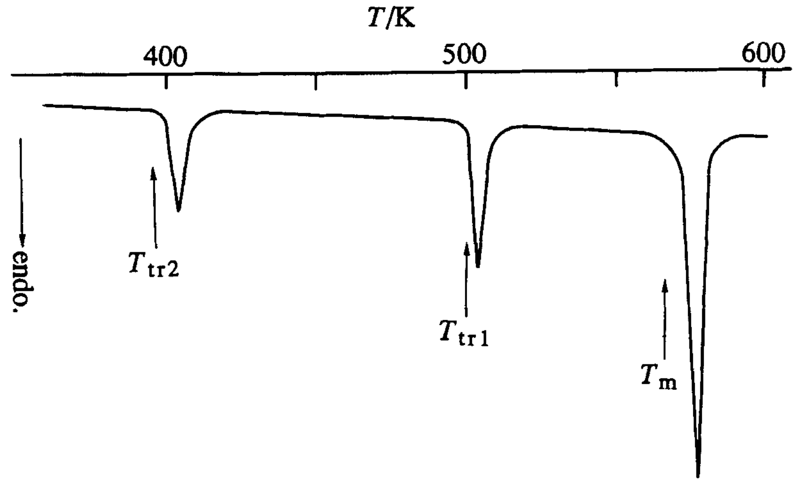

FIGURE 1 The DSC thermogram for decamethylferrocene, $[(CH_3)_5C_5]_2Fe$. T_{tr1}, T_{tr2} and T_m indicate the solid–solid phase transition and melting temperatures.

TABLE I

Observed Transition Temperatures (T_{tr}), Transition Enthalpies (ΔH) and Entropies (ΔS) in Decamethylferrocene, $[(CH_3)_5C_5]_2Fe$ Determined by Differential Scanning Calorimetry

T_{tr}/K	$\Delta H/\mathrm{kJ\ mol^{-1}}$	$\Delta S/\mathrm{J\ K^{-1}\ mol^{-1}}$
397	4.1	10
501	4.0	7.9
574*	9.2	16

* Melting point

Determined transition enthalpies (ΔH) and entropies (ΔS) are shown in Table I. The highest-temperature anomaly corresponding to the melting was observed at 574 ± 1 K(T_m) in agreement with the reported T_m of 564–568 K.[21] We hereafter call Phase I, II and III for the solid phases from the high-temperature side.

Second Moment M_2 of ^{1}H NMR Absorptions

The decay curve of the spin–echo signal can be expressed as[23]

$$F(t) \cong 1 - \frac{M_2}{2!}t^2 + \frac{M_4}{4!}t^4, \qquad (1)$$

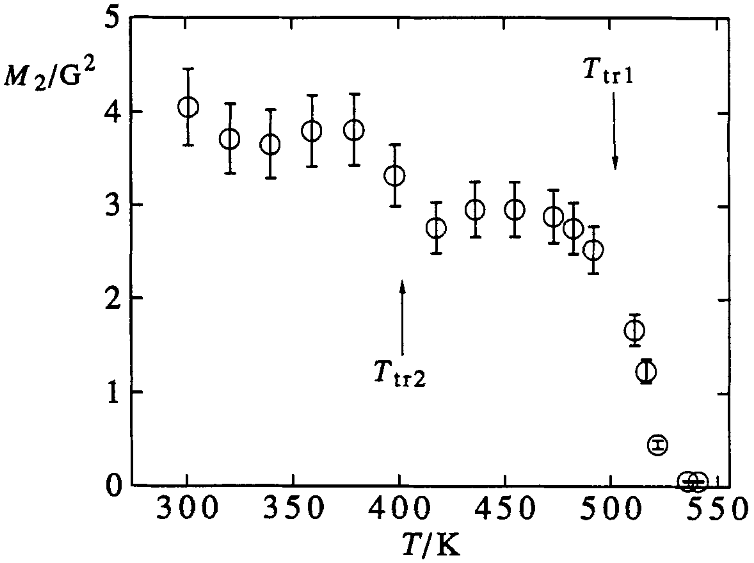

FIGURE 2 The temperature dependence of the second moment M_2 of the ^{1}H NMR line-width in decamethylferrocene, $[(CH_3)_5C_5]_2Fe$ observed above room temperature. Arrows means the phase transition temperatures.

where t and M_4 denote the time measured from the top of the echo and the forth moment of the line-width, respectively. We determined the numerical M_2 values by fitting the decay signals to Equation (1). The M_2 values obtained above room temperature are shown in Figure 2. Almost constant values of 3.7 ± 0.2 and 2.8 ± 0.1 G^2 were obtained around 350 K (Phase III) and 450 K (Phase II), respectively. Above T_{tr1}, M_2 decreased rapidly upon heating, and became ca. 0.4 G^2 at 530 K, and less than 0.1 G^2 around 540 K.

^{1}H NMR Relaxation Times T_1 and T_2

The temperature dependences of T_1 measured at Larmor frequencies of 9.45, 24.6, 36.9 and 45.8 MHz in Phase III are shown in Figure 3. Figure 4 shows T_1 data in Phase I and II measured at 9.45, 12.7, 24.6 and 45.8 MHz, and T_2 values in Phase I at 43.6 MHz. In Phase III, two T_1 minima were observed around 200 and 100 K. Upon heating, T_1 increased discontinuously at T_{tr2} and then gradually decreased in Phase II. In Phase I, a T_1 minimum was observed around 500 K and, on heating, monotonous increase of both T_1 and T_2 was observed up to 540 K where ca. 0.6 ms of T_2 was obtained.

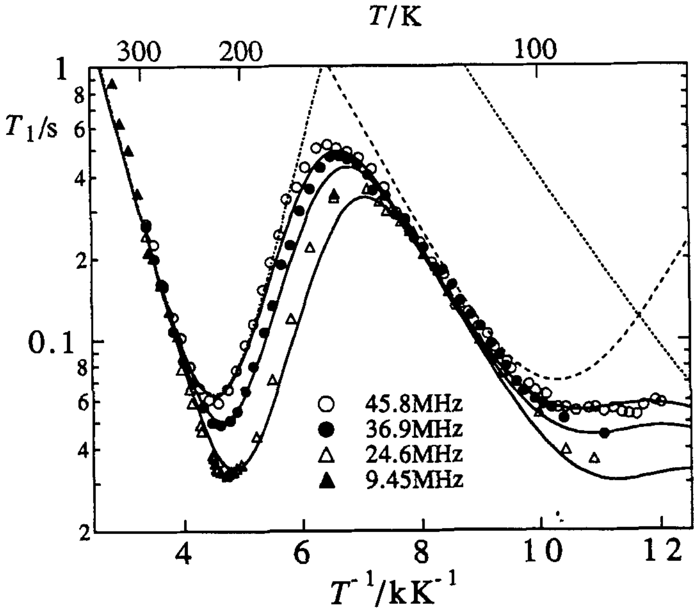

FIGURE 3 The temperature dependence of the ^{1}H NMR spin-lattice relaxation time T_1 observed in Phase III of decamethylferrocene, $[(CH_3)_5C_5]_2Fe$. The best-fitted theoretical curves (———); the contributions from T_{1Me1} and T_{1Me2} (·······, -----) and T_{1C5}(-·-·-·-·-).

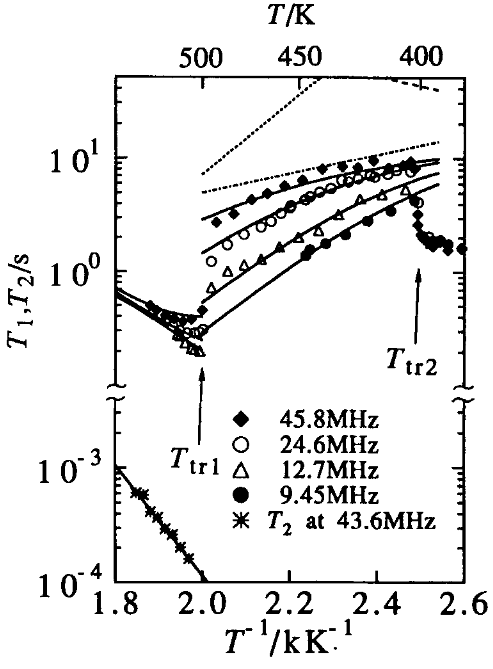

FIGURE 4 The temperature dependences of the ^{1}H NMR spin-lattice relaxation time T_1 and spin-spin relaxation time T_2 observed in Phase I and II of decamethylferrocene, $[(CH_3)_5C_5]_2Fe$. The best-fitted theoretical curves (———); the contributions from T_{1C5} (-----), T_{1Sr}(-·-·-·-·-) and T_{1nut}(·······).

DISCUSSION

Thermal Properties

The melting entropy of 16 J K^{-1} mol^{-1} determined by DSC is much smaller than that of 32 J K^{-1} mol^{-1} observed in ferrocene[24] and also smaller than the sum of the transition entropies (17.9 J K^{-1} mol^{-1}) at T_{tr1} and T_{tr2} in the present complex. It has been accepted,[25] based on experimental results on plastic crystals, that the transition entropy to the plastic phase is larger than the melting entropy, and the melting entropy of the plastic phase is less than 20 J K^{-1} mol^{-1}. The present compound satisfies these conditions, if we assume that the transition to the plastic phase takes place in two steps at T_{tr2} and T_{tr1}.

^{1}H NMR Second Moment M_2

Theoretical values of M_2 for possible motional models of decamethylferrocene were calculated using the Van Vleck's method.[26] In the calculation, we used the crystal structure determined at room temperature (Phase III).[27] Each CH_3 group is assumed to have the tetrahedral structure with the C—H distance of 1.096 Å reported for cyclohexane. For reorientating CH_3 groups about the C—C bond, the positions of three H atoms are presumed to be concentrated at the center of gravity of these atoms.

TABLE II

Theoretical and Observed Second Moments M_2 of ^1H NMR Absorptions for Possible Motional Models of Decamethylferrocene $[(CH_3)_5C_5]_2Fe$

Motional mode	Calcd. M_2/G^2	Obsd. M_2/G^2 (phase)
CH_3 rot.	10.35 (7.65 + 2.70)**	
Cp-ring C_5 rot.*	3.53(2.93 + 0.60)	3.7 ± 0.2 (III) 2.8 ± 0.1 (II)
Isotropic rot.	0.4(0.0 + 0.4)	
Self-diffusion	0.0(0.0 + 0.0)	~0.0(I)

* Cp:cyclopentadienyl

** Values in parentheses indicate the sum of intra- and intermolecular contributions in the same order.

The calculated M_2 values for four motional states are shown in Table II together with the observed value in each phase.

The value of 3.7 G^2 observed in Phase III can be well explained by the model of reorientations of CH_3 groups and both cyclopentadienyl (Cp) rings about the molecular C_5 axis, whereas 2.8 G^2 in Phase II is a little less for the C_5-reorientation model, but too high for the molecular isotropic rotation. A possible model we can propose is the nutation of the Cp-ring C_5 axis about the Fe atom by a small angle additionally taking place with the molecular C_5 reorientation. We roughly estimated the angle θ of this precessional motion about the C_5 axis using the relation given by[28]

$$M_{2\mathrm{nut}} = M^0_{2\mathrm{nut}}(3\cos^2\theta - 1)^2/4, \tag{2}$$

where $M^0_{2\mathrm{nut}}$ and $M_{2\mathrm{nut}}$ are the intramolecular M_2 with no and rapid precessional motion, respectively. The $M^0_{2\mathrm{nut}}$ is given in Table II to be 2.93 G^2 for the C_5 rotation model. The intermolecular M_2 of this precession was roughly estimated to be 0.5 G^2 by taking the average of intermolecular M_2 from the C_5 rotation and the isotropic rotation given in Table II. Setting the observed value 2.8 G^2 equal to $M_{2\mathrm{nut}} + 0.5$ G^2, the precession angle of $\theta = 16°$ was evaluated. This angle implies that the molecular packing in crystal and the site symmetry at each molecule is analogous to that in Phase III before the onset of this motion. We recorded X-ray powder diffraction patterns at ca. 420 K (Phase II) and room temperature (Phase III). These patterns are quite similar to each other suggesting that molecular site symmetries in both phases are close supporting the present model.

Just above T_{tr1}, M_2 decreased to ca. 0.4 G^2 in Phase I implying the onset of the isotropic rotation of the whole molecule. The M_2 less than 0.1 G^2 observed at ca. 540 K indicates that the molecules perform the translational self-diffusion as well as the isotropic rotation. These microscopic properties on the molecular motion are well accepted as chracteristic behavior in the plastic crystals.[29,30] From these NMR results together with the thermal data given above, Phase I can be classified into the plastic crystal.

^1H Relaxation in Phase III

The T_1 minimum observed at ca. 200 K as shown in Figure 3 can be assigned to the reorientation of both Cp rings about the molecular C_5 axis from the above M_2 analysis.

This relaxation can be expressed as[31,32]

$$T_1^{-1} = \frac{2}{3}\gamma^2 \Delta M_2 \left(\frac{\tau}{1+\omega_0^2\tau^2} + \frac{4\tau}{1+4\omega_0^2\tau^2} \right), \tag{3}$$

where γ, ΔM_2, τ, and ω_0 denote the protonic gyromagnetic ratio, the reduction of M_2 by the onset of the motion in question, the motional correlation time, and the Larmor frequency, respectively. We assume an Arrhenius-type temperature dependence of τ as given by

$$\tau = \tau_0 \exp(E_a/RT), \tag{4}$$

where E_a means the motional activation energy.

Another T_1 minimum observed around 100 K was assigned to the CH_3 reorientation about the C—C bond, which is only the possible mode expected at low temperatures. The reorientational jumping rate of each CH_3 group can be different, because three kinds of crystallographically nonequivalent CH_3 groups have been shown in Phase III.[27] In fact, the minimum value observed at ca. 100 K is much longer than the expected value for all CH_3 rotation. We tentatively tried to explain the observed data by the superposition of two BPP-type T_1 curves (T_{1Me1} and T_{1Me2}) both can be expressed by Equations (3) and (4). The experimental T_1 curve in Phase III is, accordingly, expressed as

$$T_1^{-1} = T_{1C5}^{-1} + T_{1Me1}^{-1} + T_{1Me2}^{-1}, \tag{5}$$

where T_{1C5} is the contribution from the Cp-ring C_5 reorientation. The best-fitted T_1 curves calculated by use of Equations (3)–(5) are shown in Figure 3. The determined values of unknown parameters are given in Table III. The obtained $\Delta M_2 = 6.7\,G^2$ for the high-temperature minimum agrees well with the calculated $\Delta M_2 = 6.82\,G^2$ $[= (10.35 - 3.53)\,G^2]$ from the data in Table II. The assumption of two T_1 minima was enough to explain the low-temperature data although three kinds of CH_3 groups may contribute to the relaxation. Presence of another minimum can be expected in the temperature range outside the present measurement. The activation energy of 15.9 kJ mol^{-1} for the Cp-ring C_5 reorientation is reasonable in comparison with 13.5 kJ mol^{-1} determined by the ^{13}C NMR spectra analysis.[33]

^{1}H Relaxation in Phase II

The gradual T_1 decrease with increasing temperature observed in Phase II is mainly attributable to the nutation of the molecular C_5 axis as shown in the M_2 data analysis. Assuming the condition $\omega_0\tau \gg 1$ for this motion, relaxation rate of this mechanism can be derived from Equation (3) and given by

$$T_{1\text{nut}}^{-1} \cong \tfrac{4}{3}\gamma^2 \Delta M_{2\text{nut}} \omega_0^{-2} \tau^{-1}. \tag{6}$$

The non-linearity of log T_1 vs. T^{-1} plots observed in the low-temperature range of Phase II suggests the contribution from another mechanism, which can be assigned to the Cp-ring C_5 reorientation giving the T_1 minimum in Phase III. Since, in Phase II, this motion is rapid enough fulfilling the condition $\omega_0\tau \ll 1$, the contribution of this mechanism can be written by

$$T_{1C5}^{-1} \cong \tfrac{10}{3}\gamma^2 \Delta M_{2C5}\tau. \tag{7}$$

We can see in Equation (6) that T_1 should be proportional to ω_0^2 at the high temperature range. The observed data, however, deviate from this relation indicating the contribution from the third mechanism. We assume the presence of the spin-rotation relaxation caused by the rapid Cp-ring rotation which contribution is expressed as[34]

$$T_{1Sr}^{-1} = C_{Sr}\exp(-E_{ar}/RT), \tag{8}$$

where C_{Sr} and E_{ar} are the constant depending on the spin-rotation coupling and the activation energy for the Cp-ring rotation, respectively. We expressed the observed T_1 as the superposition of Equations (6)–(8). The least-squares fitting using Equations (4) and (6)–(8) affords the best-fitted T_1 curves shown in Figure 4, and the unknown parameters as given in Table III. In the calculation, we fixed $\Delta M_2 = 6.7$ G^2 and $E_{ar} = 15.9$ kJ mol^{-1} for the Cp-ring rotation as evaluated in Phase III. The assumptions made in the calculation are supported by the result that the determined $\Delta M_2 = 1.05$ G^2 for the molecular axis nutation agrees well with the experimental $\Delta M_2 = 0.9$ G^2 [$=(3.7-2.8)$ G^2] given in Table II.

^{1}H Relaxation in Plastic Phase I

The frequency and temperature dependences of T_1 observed in Phase I were explained well by a single relaxation mechanism which we assigned to the isotropic molecular rotation by referring to the above M_2 analysis. Since a long T_2 of 0.6 ms was observed in this phase, the T_2 increase with temperature is attributable to the self-diffusion which activation energy was evaluated from the slope of the log T_2 vs. T^{-1} plot. The motional parameters of the isotropic rotation and the self-diffusion determined by the least-squares are listed in Table III, and the best fitted T_1 curves are shown in Figure 4.

TABLE III

Motional Parameters in Phase I, II and III of Decamethylferrocene, $[(CH_3)_5C_5]_2Fe$ Derived from ^{1}H Spin–Lattice and Spin–Spin Relaxation Times: Reductions of Second Moment of ^{1}H NMR Absorption (ΔM_2), Motional Activation Energies (E_a) and Motional Correlation Times at Infinite Temperature (τ_0)

Motional mode	ΔM_2/G^2	E_a/kJ mol^{-1}	τ_0/s	Phase
CH_3 rot.	6	6.2	1×10^{-13}	III
	6	7.5	2×10^{-13}	III
Cp-ring rot.	6.7	15.9	4×10^{-13}	III
	6.7*	15.9*	1×10^{-14}	II
mol. nutation	1.05	59.6	5×10^{-14}	II
Isotropic rot.	1.07	52.4	7×10^{-15}	I
Self-diffusion	0.4**	93.1	2×10^{-15}	I

* Assumed the same values determined in Phase III

**Calculated value from data in Table II.

The activation energies in Phase I are comparable with 66.5 kJ mol^{-1} for the combined motion of the isotropic rotation and the self-diffusion in the plastic phase of formylferrocene[4], and 152 and 96.4 kJ mol^{-1} for the self-diffusion in the plastic phase of adamantan[35] and triethylenediamine,[36] respectively, which have roughly the same molecular size as of the present molecule.

It is widely accepted in plastic crystals that the diffusional correlation time τ at the extrapolated T_m falls into a narrow range of ca. 10^{-7} s.[29,30] This relation has been shown in many plastic crystals of molecular compounds. Recently, we have revealed that, in the plastic phase of ionic crystals[37] and in the two-dimensional plastic crystals,[38] the same characteristic time of ca. 10^{-7} s can be observed at the respective T_m. In the present compound, this time became 5.9×10^{-7} s at T_m. This value also comes to the same range of values so far reported.

References

1. C. H. Holm and J. A. Ibers, *J. Chem. Phys.*, **30**, 885 (1959).
2. A. Kubo, R. Ikeda and D. Nakamura, *Chem. Lett.*, 1497 (1981).
3. A. Kubo, R. Ikeda and D. Nakamura, *Chem. Lett.*, 1487 (1982).
4. A. Kubo, R. Ikeda and D. Nakamura, *Ber. Bunsenges. Phys. Chem.*, **90**, 479 (1986).
5. A. Kubo, R. Ikeda and D. Nakamura, *J. Chem. Soc., Faraday Trans 2*, **82** 1543 (1986).
6. A. Kubo, R. Ikeda and D. Nakamura, *Z. Naturforsch.*, **43a**, 78 (1988).
7. F. Y. Uchimi, Y. Masuda, K. Iwai, M. Katada and H. Sano, *Hyperfine Interactions*, **42**, 1091 (1988).
8. K. Sato, M. Iwai, H. Sano and M. Konno, *Bull. Chem. Soc., Japan*, **57**, 634 (1984).
9. K. Sato, M. Konno and H. Sano, *Chem. Lett.*, 17 (1984).
10. K. Sato, M. Katada, H. Sano and M. Konno, *Bull. Chem. Soc., Japan*, **57**, 2361 (1984).
11. J. W. Edwards, G. L. Kington and R. Mason, *Trans. Faraday Soc.*, **56**, 660 (1960).
12. K. Ogasahara, M. Sorai and H. Suga, *Chem. Phys. Lett.*, **68**, 457 (1979).
13. K. Ogasahara, M. Sorai and H. Suga, *Mol. Cryst. Liq. Cryst.*, **71**, 189 (1981).
14. M. Naruse, M. Sorai and M. Sakiyama, *Mol. Cryst. Liq. Cryst.*, **101**, 219 (1983).
15. M. Sorai and Y. Shiomi, *Mol. Cryst. Liq. Cryst.*, **107**, 271 (1984).
16. K. Chhor, C. Pommier and M. Diot, *J. Chem. Thermodyn.*, **16**, 503 (1984).
17. M. Sorai and Y. Shiomi, *Thermochim. Acta*, **109**, 29 (1986).
18. M. Nakano and M. Sorai, *Chem. Phys. Lett.*, **169**, 27 (1990).
19. M. D. Lowery, R. J. Wittebort, M. Sorai and D. N. Hendrickson, *J. Am. Chem. Soc.*, **112**, 4214 (1990).
20. T. J. Kealy and P. L. Pauson, *Nature*, **168**, 1039 (1951).
21. R. B. King and M. B. Bisnette, *J. Organometal. Chem.*, **8**, 287 (1967).
22. Y. Kume, R. Ikeda and D. Nakamura, *J. Magn. Reson.*, **33**, 331 (1979).
23. J. G. Powles and J. H. Strange, *Proc. Phys. Soc.*, **82**, 6 (1963).
24. unpublished data.
25. J. Timmermans, *J. Phys. Chem. Solids.*, **18**, 1 (1961).
26. J. H. Van Vleck, *Phys. Rev.*, **74**, 1168 (1948).
27. D. P. Freyberg, J. L. Robbins, K. N. Raymond and J. C. Smart, *J. Am. Chem. Soc.*, **101**, 892 (1979).
28. H. S. Gutowsky and G. E. Pake, *J. Chem. Phys.*, **18**, 162 (1950).
29. J. M. Chezeau and J. H. Strange, *Phys. Rep.*, **53**, 1 (1979).
30. N. Boden, "The Plastically Crystalline State", Ed. J. N. Sherwood, Wiley, Chichester, 1979. p. 147.
31. N. Bloembergen, E. M. Purcell and R. V. Pound, *Phys. Rev.*, **73**, 679 (1948).
32. G. Soda and H. Chihara, *J. Phys. Soc. Japan.*, **36**, 954 (1974).
33. D. E. Wemmer, D. J. Ruben and A. Pines, *J. Am. Chem. Soc.*, **103**, 28 (1981).
34. P. S. Hubbard, *Phys. Rev.*, **131**, 1155 (1963).
35. H. A. Resing, *Mol. Cryst. Liq. Cryst.*, **9**, 101 (1969).
36. R. Folland, R. L. Jackson, J. H. Strange and A. V. Chadwick, *J. Phys. Chem. Solid*, **34**, 1713 (1973).
37. M. Tansho, D. Nakamura and R. Ikeda, *Ber. Bunsenges. Phys. Chem.*, **95**, 1643 (1991) and references therein.
38. M. Hattori, S. Fukada, D. Nakamura and R. Ikeda, *J. Chem. Soc. Faraday Trans.*, **86**, 3777 (1990).